

First Detailed Observations of Discharges within the Artificial Charged Aerosol Cloud

M. G. Andreev¹, N.A. Bogatov⁴, A. Yu. Kostinskiy^{2,4,*}, L. M. Makal'sky³,
E. A. Mareev⁴, D.I. Sukharevsky^{1,4}, V. S. Syssoev^{1,4}

1. High-Voltage Research Center of the All-Russia Institute of Electrical Engineering, Istra, Moscow region, Russia
2. National Research University Higher School of Economics, Moscow, Russia
3. Power Engineering University of Moscow, Russia
4. Institute of Applied Physics of the Russian Academy of Sciences, Nizhny Novgorod, Russia

ABSTRACT: We have observed for the first time the intracloud discharge with plasma parameters close to the parameters recorded in the long spark discharges. Plasma structures occurred in the artificial highly charged aerosol clouds of the negative and positive polarities. These plasma structures were recorded with the use of a high-speed IR camera (of wavelength 3.8-4.9 μm) simultaneously with the visible radiation recorded by high-speed visible cameras and photomultiplier tubes (PMTs) with interference filters. The wavelength range of the IR camera gave to us a unique possibility for diagnostics of the structures within the cloud formed by drops with a typical radius of 0.5 μm . The plasma structures found in the positive and negative clouds differ substantially. Elongated discharge channels are often organized into different clusters of the complicated structure. The thermal-ionization instability is discussed as a common mechanism of the plasma channel formation in the observed discharges and the natural cloud and cloud-to-ground discharges.

INTRODUCTION

Long sparks more than 1 m long, which start from the conductive object towering above the grounded plane in the field of an artificially created cloud of charged water aerosol (droplets) were obtained by the co-authors of this work a long time ago [Vereshchagin et al., 1986; Antsupov et al., 1990].

The setup for a study of discharges within the charged water aerosol cloud has been specially chosen and prepared. Charged aerosol cloud is fundamentally different from any arbitrarily powerful high-voltage electrode system in that it is among the natural aerosol systems, such as a storm cloud, tornado, volcanic charged dust, etc. In all of these systems the charge is on the dispersed particles, and for the implementation of the discharge it is necessary that during the discharge, part of the charge is removed from the aerosol by some rapid collective process. Thus, an artificially charged aerosol cloud is a small (a few tens of cubic meters), but full-fledged member of the family of charged aerosols that generate long spark discharges of the positive and negative polarities. The intracloud processes in the initiation and

* Contact information: A. Yu. Kostinsky, National Research University Higher School of Economics, Moscow, Russia, Email: kostinsky@gmail.com, akostinsky@hse.ru.

propagation of long and super-long sparks (lightning) in aerosol discharges are the most difficult to understand since a cloud aerosol of large size from 3-5 μm to several millimeters precludes the use of well-proven methods of measurements in the visible and IR ranges, including the spectral ones. In recent decades, very effective VHF systems have successfully been used (e.g., [Edens et al., 2012]), but the nature of the radio-emitting objects remains to be better understood. Therefore, any new experimental information about the processes in artificially charged aerosols, where the particle size can be specified, is of great interest. From these considerations, we use charged aqueous aerosols with an average size of 0.5 μm to "see" inside the cloud through modern infrared cameras with the matrices that are sensitive in the wavelength range of 3-14 μm (mid-IR). This combination of aerosol parameters and parameters of the diagnostic radiation has shown that within the charged aerosol cloud there are several classes of new intracloud plasma objects that are very likely to have counterparts both in the lightning discharges and in the discharges generated by volcanoes, tornadoes, and dust storms. In this paper, we will describe plasma objects detected in the water aerosol cloud of the negative polarity.

EXPERIMENTAL SETUP

The layout of the experimental setup we use in this paper is similar to that described in [Vereshchagin et al., 1986; Antsupov et al., 1990] and is intended for generation of the charged cloud of the negative and positive polarities (Fig. 1). Outlet nozzle (2.3) of the charged aerosol generator was located at the center of a flat metal screen 2 m in diameter, with rounded edges (3). The charged aerosol generator consisted of a steam generator (2.1) and a charger (2.2). Steam-air jet from the steam conductor at a temperature of about 100-120 $^{\circ}\text{C}$ under a pressure of 0.2-0.6 MPa flew out at a speed close to the speed of sound in the mixture (about 400-450 m/s) from the nozzle (2.3) with an aperture angle of 28° , forming an adiabatically expanding submerged jet. In such a way, a charged aerosol cloud (1) was created in the atmosphere. As a result of rapid cooling, the steam condensed into drops of about 0.5-1 μm . This fact, as was noted in the Introduction, is very important for these experiments because the drop sizes are an order of magnitude smaller than the range of sensitivity of an IR camera that "sees" in the IR range in almost the entire volume of the cloud interior. The ions charging the aerosol were formed in the corona discharge between a thin pointed needle located in the nozzle (2.3) and the nozzle. A negative-polarity DC voltage of 10 - 20 kV was fed to the needle from a high-voltage source (2.2). The current of discharge removal by the air-steam jet lied in the range 60-150 μA . Various discharges occurred spontaneously as a total charge of up to about 60 μC accumulated in the droplets.

The current was measured using a shunt with 1- Ω resistance. The signal from the shunt was fed to the Tektronix DPO, a digital oscilloscope with 500-MHz band (13). The shunt was connected to the receiving electrode in the form of a metal ball (4), 5 cm in diameter, with the highest point 12 cm above the flat screen. The ball was located at a distance of 0.8-0.9 m from the ball center. When the current in the shunt exceeded a given value, the oscilloscope was run, which, in turn, gave a pulse to launch 4 Picos (9), a high-speed visible camera, and FLIR7700M (10), an IR camera. For dynamic control of the total charge of the aerosol cloud, we used an insulated copper ball (6), 50 cm in diameter, connected via a 100-M Ω resistor to oscilloscope (13). This allowed us to record the dynamics of the charge accumulation in the cloud charging and the fast processes of the charge escape from the cloud. The ball is at a distance of 6 m from the aerosol cloud. To measure fast processes in the visible range, we used a PMT (11) with

interference and bandpass filters, which selected a spectral range characteristic of the radiation of long streamers in the air (300-440 nm) and a spectral range where the streamer radiation is absent (500-560 nm), but there is strong radiation of discharges with high number density and temperature of the electrons (in particular, spark discharges). This allowed us to distinguish, in a first approximation, the classical streamer corona from spark discharges and other plasma structures with a high gas temperature. The overall picture of the discharge was recorded with Canon (12), a color digital camera. The electric field at the surface of the grounded plane was measured by a flux meter (5).

DETECTION OF NEW PLASMA INTRACLOUD FORMATIONS -- *STALKERS*

Figure 2 shows a typical integrated photograph of discharges in the visible range with 5-s exposure. Four positive discharges rising from the ball are seen. The discharges followed each other once per second on the average. It seems that in this case nothing happens in the aerosol cloud.

Figure 3 (a, b) shows two consecutive frames taken by an IR camera, which record the upper, hidden part of the upward discharge in the cloud (such as the discharges in Fig. 2). Each frame was taken with 7-ms exposure. The time between frames was 1.7 ms. The upper part of the tortuous channel of the positive spark discharge (1) rising from the ball to the cloud, with the current passed through the shunt, is well seen on the bottom of Fig. 3a in the middle. An oscillogram of this current is given in Fig. 4 (yellow curve). After the flare of the streamer corona, the positive leader began to move up. The discharge lasted about 35 μ s. During the discharge, the total charge of the cloud decreased in proportion to the leader current, as is indicated by the green curve in the oscillogram of Fig. 4, which measures the current from an uncalibrated insulated copper ball of 50 cm in diameter. The central part of the leader channel is heated to several thousand degrees [Bazelyan and Raizer, 1997; Les Renardières Group, 1977], and therefore the channel on the IR image (Fig. 3) looks like a bright, tortuous, branching line. This discharge is similar to the positive lightning discharge rising from high buildings to the negative edge of the natural cloud in the case where no return strokes follow [Rakov and Uman, 2003]. The spark channel in Fig. 3a is within the flux of streamers (2).

However, the new bulk plasma structures (objects) (3) in Fig. 3a, which were detected for the first time inside the cloud, are of the greatest interest. These structures are very difficult to be attributed to the spark discharge that follows the path of the leader channel or to the long streamers. Comparison of the intensity of the infrared radiation coming from the bulk plasma structures and from the spark channel in this frame shows that the new plasma structures have on the average the same radiation intensity in the IR range as the spark channel heated to several thousand degrees [Bazelyan and Raizer, 1997; Les Renardières Group, 1977] and are an order of magnitude greater than the streamer radiation. Moreover, in the next frame (7) taken with 7-ms exposure, which follows in 1.7 ms (Fig. 3b), new plasma structures radiate even more strongly than the spark channel. It is important to note that the new plasma structures in these frames form an hierarchical system and cannot be attributed to the bidirectional leader [Kazemir, 1960]. Three brightest channels 25-30 cm long are slightly tortuous and electric field oriented, as well as the streamer corona. Weaker spindle-shaped plasma structures (objects) branch off from these channels. The radiation intensity of these plasma structures in the IR range is 3-5 times lower than that of the brightest plasma structures (objects). Due to these secondary channels, bright plasma structures are intertwined and interact with long streamers of the corona. The plasma structures branch towards the spark

channel. It can also be noted that the lower bright plasma structure interacts with the upward spark discharge through the streamer zone before reaching the spark channel 3-4 cm long. Their interaction is manifested in the greater blackening and structuring of the streamer zone near the top of the spark channel.

The event recorded in the IR range and shown in Fig. 3a,b, as well as its oscillogram given in Fig. 4, are typical of the positive charge rising into the negative aerosol cloud. More than a hundred of such events in the IR range with new plasma structures have been recorded, and thousands of similar oscillograms of the upward positive leader have been observed [Vereshchagin et al., 1986; Antsupov et al., 1990].

For brevity's sake we will call these new intracloud plasma structures *stalkers*. Stalk is a synonym for the word stem, or trunk, etc. Stems and stalkers are probably of the same nature.

THE VARIETY OF STALKERS

Stalkers are formed and interact not only with the tops of the positive spark channels and are formed not only about the axis of the aerosol jet. They can be found throughout the entire volume of the aerosol cloud, and they can be of various length and structure, but each structure has bright luminous kernels (channels) close to the spark channel in brightness of the IR radiation, which is evidence for strong heating of the *stalkers*.

Figure 5 shows an important class of detected *stalkers* – *the stalkers* located along the spark discharge and interacting through the streamer corona with lower branches of the spark channel rising to the negative cloud. Fine structure of the *stalker* is clearly seen in Fig 5. Long positive streamers branch off towards the cloud from the *stalker's* bright kernel 3-4 cm long up to the negative cloud (as to the flat negative electrode) and short negative streamers branch off down towards the branch of the positive spark channel (as to the stem positive electrode). The picture is very similar to the stem of the negative leader with the positive and negative streamers branching off from it [Stekolnikov et al., 1962; Les Renardières Group, 1981; Gorin and Shkilev, 1976; Biagi et al., 2010].

An important feature of *stalkers* is that they can form spatial systems that interact among themselves and with the channel of the upward leader, due to the positive and negative streamers. This is clearly seen in Fig. 6 showing two *stalkers* located at a distance from each other. The small *stalker* with a 5.7-cm kernel (similar to the stem of the negative leader) is in parallel, just above the center of the spark channel and interacts through the negative streamers with the bottom of the spark channel, while the positive streamers interact with other, higher lying *stalkers* that are closer to the jet axis and are similar to the *stalkers* shown in Figs. 3 and 5. The top of the upward spark channel also interacts with the upper *stalkers* through its streamer system, as in Figs. 3 and 5. Dozens of such events have been detected to date.

Two questions arise: “How much are the *stalkers* connected with the spark channel?” and “Can they exist without it?” We found several dozens of events where stalkers appear in the aerosol cloud independently, as separate phenomena, even without the presence of the upward spark discharge. Examples can be seen in Figs. 7 and 8. Both phenomena were recorded near the grounded plane. In Fig. 7, the *stalkers* branch up and in Fig. 8 they branch down and have a spindle structure similar to the *stalkers* in Figs. 3 and 5.

The variety of "types" of *stalkers* and their interaction with each other makes us look for the root

cause of the appearance of *stalkers*. Maybe *stalkers* are the manifestation of another, more general collective process in the aerosol cloud? We began to systematically scan the aerosol cloud, starting with the ball and rising with each successive frame 50 cm above and 20 cm to the left of the center of the aerosol jet. A tortuous, branching positive leader rising from the ball, and positive streamers around it, are seen in Fig. 9. *Stalkers* are not visible in this picture. In the next step, looking above and to the left, we see in Fig. 10 the upper part of the upward positive leader (lower right corner) and *stalkers* in the upper left corner as a "broom" branching down and streamers connecting the *stalkers* and the spark channel. In the next step, raising the camera angle even higher and to the left, we stop to record the upward spark channel and see only the "broom" of *stalkers* that is close to the axis of the charged aerosol jet (Fig. 11). Finally, rising even higher and further to the left, we see in the frame the whole central part of the aerosol jet in Fig. 12. In the right frame of Fig. 12b it is seen that *stalkers* in the form of a broom branching up reach the jet axis and do not cross it, while in the left frame of Fig. 12a it is seen that a positive spark discharge and *stalkers* rise from the other side of the jet without crossing it. Thus, from the entire set of frames given in Figs. 9-12 it can be assumed that *stalkers* represent exactly all the "intracloud life" of the aerosol cloud. Other structures have not been detected to date.

OBSERVATION OF STALKERS IN THE VISIBLE RANGE

Is it possible to record *stalkers* simultaneously in the visible and mid-IR ranges? Such measurements in the visible range are complicated by the fact that for the drop size of about 0.5 μm , visible light has a wavelength close to the size of the drops and is effectively scattered by them. The images, if obtained, are often vague and lack contrast. Despite this, we were able to simultaneously record *stalkers* in the visible and mid-IR ranges. Possibly, the *stalkers* were near the edge of the clouds and the optical density of the aerosol layer before a 4 Picos high-speed camera was low. A visible image of *stalkers* in Fig. 13 was recorded by a 4 Picos camera aimed at the center of the aerosol clouds at a height of 80-120 cm above the plane where the ball is located. The camera was started from the current pulse coming from the ball through the shunt 400 ns after the initial flare of the corona. The exposure time was 1 μs . The picture is fuzzy but is clearly distinguishable since the *stalkers* are inside the cloud.

Figure 15 shows simultaneously an IR image of the same event as in Fig. 13 with 8-ms exposure. In the upper left corner of Fig. 14, for clarity, Fig. 13 shows a fragment depicting *stalkers* in the visible range. It is seen that the contours of the brightest *stalkers* are similar in the visible and near-IR images. The significant brightness superiority of one of the *stalkers* (the right-hand one) in the IR photographs can be attributed to its further development after the closing of the optical shutter of the 4 Picos camera.

For clarity, we also give two more examples of the visible image of *stalkers*. The viewing field in Fig. 15 taken by a 4 Picos camera comprises both the starting leader with the streamer corona rising from the leader and much brighter plasma structures on the top of the streamer corona, which can be *stalkers*. Since about 1.5 μs passed from the start of the discharge, the leader has developed only by a few centimeters. In the next Fig. 16, *stalkers* are quite clearly seen. The picture was taken 1 μs after the discharge. The exposure time was 200 ns. In brightness, *stalkers* are only slightly different from the leader channels. They arose long before the leader was able to develop, and this plasma structure cannot be its continuation.

As a result, it can be stated that with high probability, the *stalkers* were recorded not only in the mid-IR range, but also in the visible range.

DISCUSSION OF EXPERIMENTAL RESULTS

This paper describes for the first time new plasma structures (which we termed *stalkers*) detected during discharges in the cloud of a negatively charged aqueous aerosol. It appears that *stalkers* are not rare occurrences. Conversely, with appropriate techniques, they can be found almost in each intracloud discharge, of both positive and negative polarities.

It is important to emphasize that there is a significant number of events where *stalkers appear separately from the upward positive discharges and are in no way related to them* (Figs. 7 and 9). This indicates that the formation of hot extended plasma channels, at least in a certain class of events, is an independent, not only secondary process initiated by the leaders of a long spark. Moreover, in the second part of this work, which is dedicated to the positively charged cloud, we discuss the events in which, figuratively speaking, the *stalkers* themselves are the “cause” of the positive and negative leaders. Thus, at least for some events, the *stalkers* are primary and the leaders are secondary phenomena. *Stalkers* (at least many of them) are with high probability neither positive nor negative leaders or streamers. *Stalkers* cannot be considered streamers because they radiate in the spectral ranges where they highlight only hot channels (the measurement results will be presented elsewhere), and streamers in these ranges do not have any significant emission of molecular bands and atomic lines under atmospheric pressure. This leads to the hypothesis that *stalkers* are separate plasma objects *with their own physical mechanism of formation*.

In our view, a significant role in explaining the causes of the appearance of *stalkers* could be played by the thermal-ionization instability mechanism, which is responsible for the heated plasma structures in significantly sub-threshold fields. The mechanism of the thermal-ionization instability can lead to a contraction of the channels and their significant heating in the existing fields, too, if disturbances of the air density and/or electric field and/or electron density sufficient to overcome the instability threshold can occur in the surrounding air. These disturbances may include strong turbulence in the region of the thunderstorm cell, air density disturbances during passage through the leader branch (recoil leader), air density and electron number density disturbances during the passage of a streamer or, more probably, a few streamers along the same channel, followed by the development of thermal instability and contraction, as was observed in the experiment [Starikovskiy et al., 2010].

The comparison of the stem and the volume leader of a long negative spark or lightning [Gorin and Shkilev, 1976; Les Renardières Group, 1981; Biagi et al., 2010; Petersen et al., 2008] with the results obtained in this paper raises the question about similarity of these phenomena occurring in the sub-threshold fields in the air. Interestingly, the treatment of initial lightning leader formation by analogy with the formation of a space leader in a laboratory negative stepped leader suggested by [Petersen et al., 2008] allowed them suggesting the hypothetical schematics (Figure 8 in [Petersen et al., 2008]) which look very similar to some of our experimental pictures.

It should be noted that the phenomena observed in the aerosol cloud (see, e.g., Figure 5) can be similar also to such processes (which are observed and discussed concerning intracloud discharge problem) as a recoil leader and a recoil streamer [Mazur et al., 2011] (see also [Edens et al., 2012]), which occur in sub-threshold fields along the contracted channel of the negative and positive leaders. The latter can radiate strong ultraviolet in the channel vicinity, as well as stimulate, by their strong electric field, the

development of instability in the former leader channels close to them, in which the gas density is much lower because of the heating, and the E/N ratio is greater than in the surrounding air. It would be useful to consider such processes also in terms of thermal-ionization instability mechanism implication.

Finally, the bulk network of *stalkers* (plasma structures interacting with each other through positive and negative streamers) can serve as a model of the physical mechanism of metallization of a storm cloud [Iudin et al., 2003]. Due to a strong heating in the areas where the contraction followed the mechanism of the thermal-ionization instability, the network of plasma channels may exist for a long time and expand without sticking to a fast electron recombination that occurs in the streamers. Such a network, when expanding, may acquire great capacitance and a sufficient potential to start a classical leader process.

Note again that this paper presents the data on intracloud discharges only for the negative aerosol cloud. A large generation of *stalkers* has also been detected in the positively charged aerosol cloud.

ACKNOWLEDGMENTS

The authors thank Stanislav Davydenko, Nikolay Ilyin, Dmitry Iudin, Vladimir Klimenko, Vladimir Rakov, Yuriy Shlyugaev and Nikolay Slyunyaev for useful discussions and are grateful to the Ministry of Education and Science of the Russian Federation for the financial support (project No. 14.B25.31.0023).

REFERENCES

- Antsupov, K. V., I. P. Vereshchagin, M. A. Koshelev, A. V. Lupeiko, L. M. Makal'sky, V. S. Syssoev, and E. N. Chernov, Study of spark discharges from the cloud of aerosol particles, *Izv. Akad. Nauk SSSR, Energetika i Transport* (in Russian), No.4, pp.158–162 (1990).
- Bazelyan, E. M., Yu. P. Raizer. *Spark Discharge*. CRC Press, 1997.
- Biagi, C. J., M. A. Uman, J. D. Hill, D. M. Jordan, V. A. Rakov, and J. Dwyer, Observations of stepping mechanisms in a rocket-and-wire triggered lightning flash, *J. Geophys. Res.*, 115, D23215 (2010).
- Gorin, B. N. and A. V. Shkilev, The development of electrical discharge in long gaps rod-plane with a negative voltage pulse, *Elektrichestvo* (in Russian), No.6, pp.31–39 (1976).
- Edens, H. E., K. B. Eack, E. M. Eastvedt, J. J. Trueblood, W. P. Winn, P. R. Krehbiel, G. D. Aulich, S. J. Hunyady, W. C. Murray, W. Rison, S. A. Behnke, and R. J. Thomas, VHF lightning mapping observations of a triggered lightning flash, *Geophys. Res. Lett.*, 39, Issue 19 (16 October 2012).
- Iudin, D.I., V. Yu. Trakhtengerts, and M. Hayakava, Fractal dynamics of electric discharges in a thundercloud, *Physical Review E*, 68, 016601 (2003).
- Kasemir, H. W., A contribution to the electrostatic theory of a lightning discharge, *J. Geophys. Res.* 65, pp. 1873–1878 (1960).
- Mazur, V., L. H. Ruhnke, T. A. Warner, and R.E. Orville, Discovering the Nature of Recoil Leaders, XIV ICAE, August 08–12, 2011, Rio de Janeiro, Brazil.
- Petersen, D., M. Bailey, W. H. Beasley, and J. Hallett, A brief review of the problem of lightning initiation and a hypothesis of initial lightning leader formation, *J. Geophys. Res.*, 113, D17205 (2008).
- Rakov, V. and M. Uman. *Lightning: Physics and Effects*. Cambridge Univ. Press, 2003.
- Raizer, Y. P. *Gas Discharge Physics*. Springer-Verlag, 1991.
- Les Renardières Group, Positive discharges in long air gaps—1975 results and conclusions. *Electra*, 53, pp. 31–132

(1977).

Les Renardières Group, Negative discharges in long air gaps. *Electra*, 74, pp. 67–216 (1981).

Stekolnikov, I. S. and A. V. Shkilev, New materials on the development of negative spark and its comparison with the lightning, *Dokl. Akad. Nauk SSSR* (in Russian), Vol.145, No.4, p.782–785 (1962).

Starikovskiy, A. Yu., A. E. Rakitin, and S. V. Pancheshnyi, Periodic pulse discharge self-focusing and streamer-to-spark transition in under-critical electric field, 63rd Annual Gaseous Electronics Conference, 55, No. 7, October 4–8, 2010, Paris, France.

Vereshchagin, I. P., M. A. Koshelev, L. M. Makal'sky, and V. S. Syssoev, Preliminary results of using a charged aerosol generator for modeling of atmospheric discharges, in: *Proc. of the Third All-Union Symp. on Atmospheric Electricity* (in Russian), Tartu, 1986. *Gidrometeoizdat, Leningrad* (1988), pp.119–123.

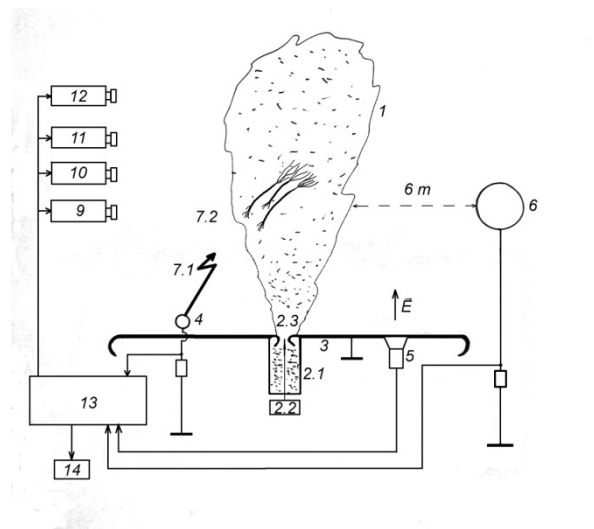


Fig. 1. Layout of the experiment. 1 - the cloud of charged aerosol; 2.1 - steam-air jet generator; 2.2 - the source of high voltage applied to the needle in the nozzle; 2.3 - the nozzle through which the steam-air jet with corona needle in the middle is output; 3 - grounded metal plane; 4 - receiving electrode (a metal ball of 5 cm in diameter); 5 – slow electric field meter (flux meter); 6 – fast electric field probe (a metal ball of 50 cm in diameter); 7.1 - upward positive leader; 7.2 - downward negative leader; 9 - FastCam SA4 high-speed video camera; 10 - FLIR 7700M high-speed IR camera; 11 - PMT; 12 – photo camera; 13 – signal synchronization and recording unit (Tektronix DPO 71004 oscilloscope and Tektronix AFG 3252 signal generator); 14 - data storage unit (PC).



Fig. 2. Integrated photograph of discharges with 5-s exposure. Four upward positive discharges from the ball, which is connected through the shunt to the oscilloscope.

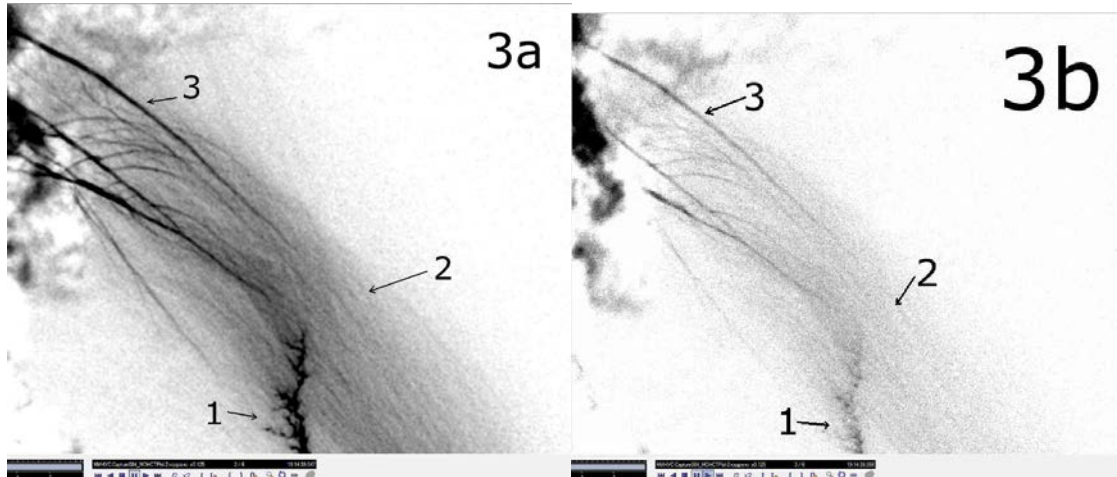


Fig. 3. Two successive frames (a, the first and b, the second) taken by an IR camera, which records the upper (hidden by the aerosol) part of the upward discharge. Exposure time is 7 ms. The time between frames is 1.7 ms. The number of pixels in each frame is 640x520. All events recorded in the frame occurred inside the cloud of charged aerosol. Only flares of scattered radiation are seen in the visible range in this experiment. 1 – the channel of the upward discharge, 2 - streamer corona, 3 - intracloud plasma structures.

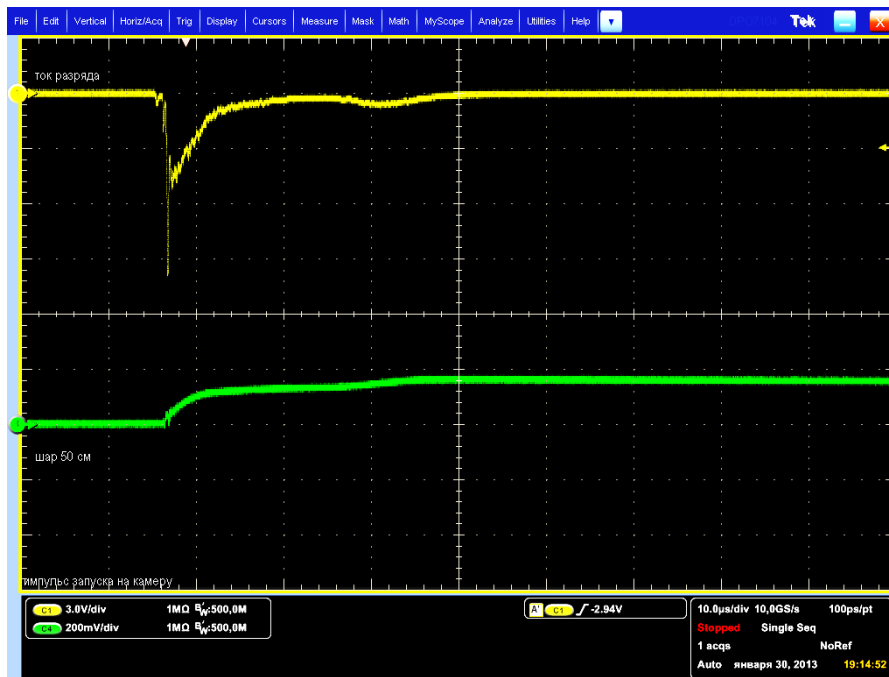


Fig. 4. Oscillogram of the events recorded in Fig. 3. The upper (yellow) curve – the current of the upward positive leader going through the shunt (one large vertical division corresponds to the current 1 A and one large horizontal division corresponds to the time interval 10 μ s). The lower (green) curve shows the charge escape from the cloud (the instrument is not calibrated and is used for a qualitative understanding of the processes of the charge escape from the cloud).

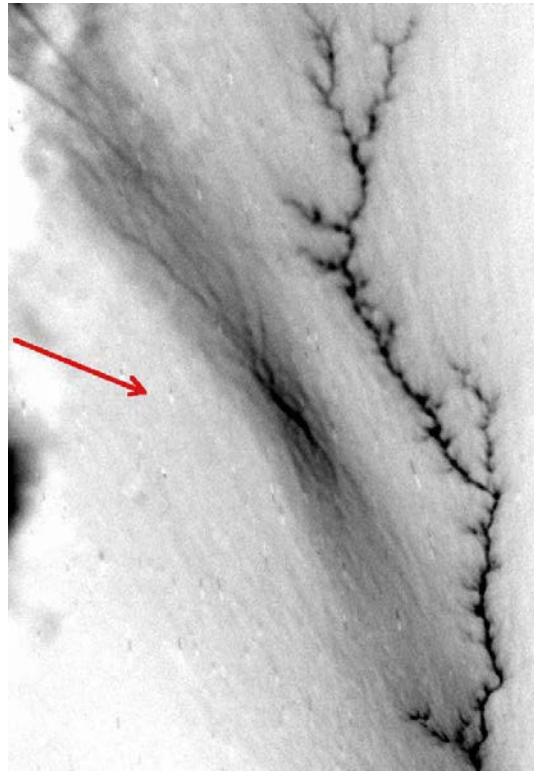


Fig. 5. The frame taken by an IR camera, which records the upper (hidden partially by the aerosol) part of the upward channel (right). The *stalker* is in the middle of the frame. Exposure time is 7 ms.

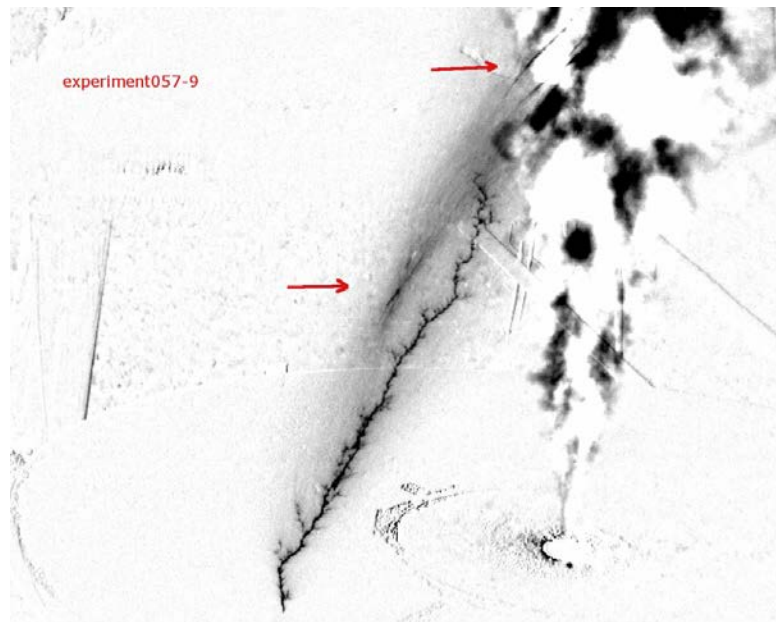


Fig.6. Two *stalkers* spaced apart. The positive discharge channel is about 1 m long.

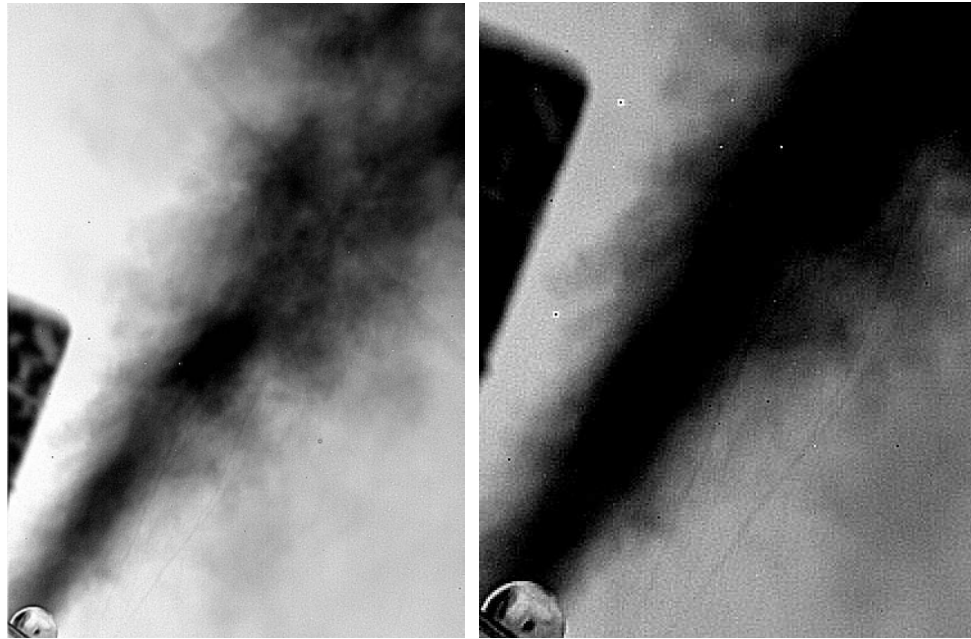


Fig. 7. The *stalkers* recorded in the aerosol cloud as separate phenomena, without the upward spark discharge. The *stalkers* are branching up. The right frame is the scaled-up part of the left frame. The ball diameter is 5 cm.

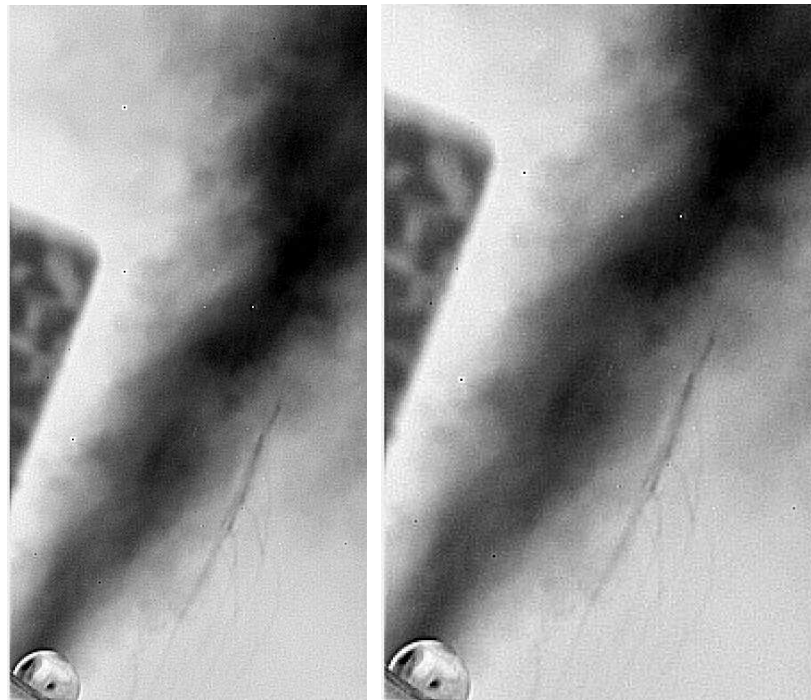


Fig. 8. The *stalkers* recorded in the aerosol cloud as separate phenomena, without the upward spark discharge. The *stalkers* branch down. The right frame is the scaled-up part of the left frame. The ball diameter is 5 cm.



Fig. 9. The tenuous, branching, positive upward leader and the positive streamers around it, climbing to the cloud. The *stalkers* are not seen in this frame.

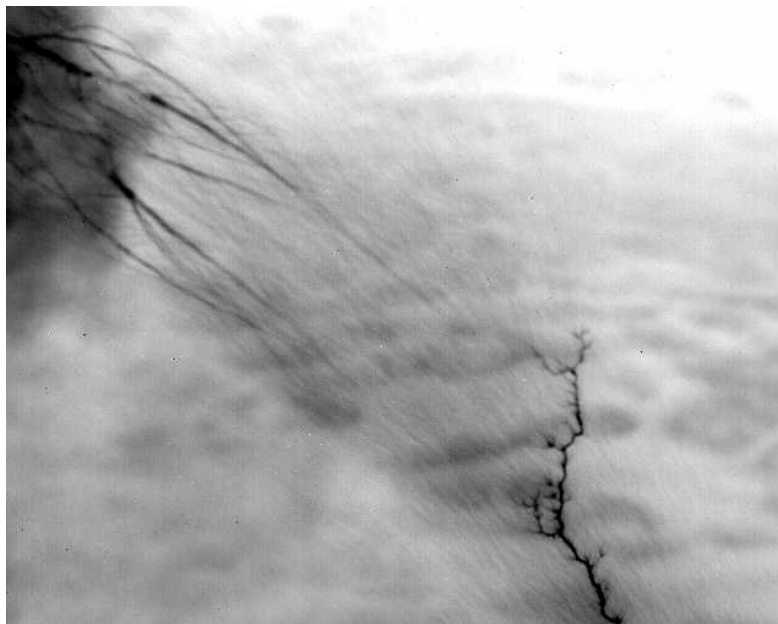


Fig. 10. Upper part of the upward positive leader (bottom right), *stalkers* in the form of a broom (upper left corner) and connecting the *stalkers* and the spark channel - *streamers*. Heat release generation in the brightest branches of the broom is very irregular. The frame was recorded by an IR camera. Exposure time is 7 ms. The number of pixels in each frame is 640x520.

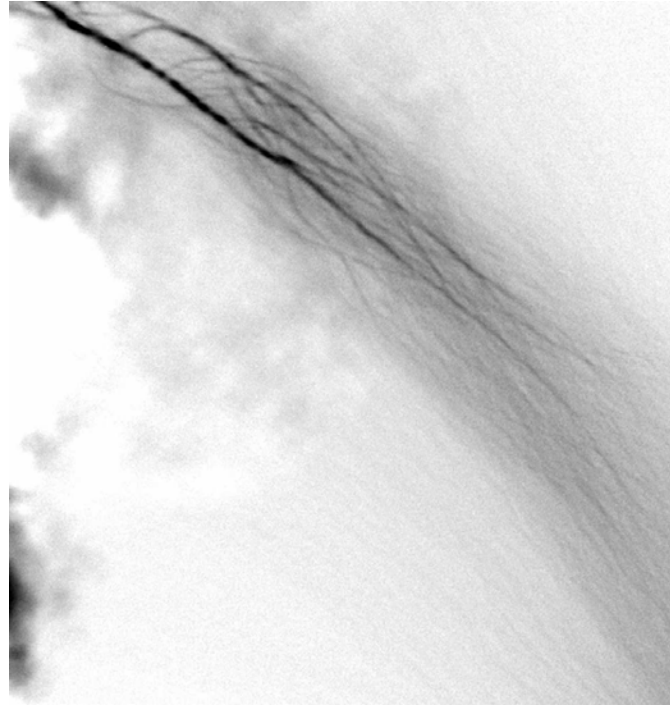


Fig. 11. Only the *stalkers* in the form of a broom (upper left corner) and those connecting the *stalkers* and the spark channel (not seen because of the lower location). The frame recorded by an IR camera. Exposure time is 7 ms. The number of pixels in each frame is 640x520.

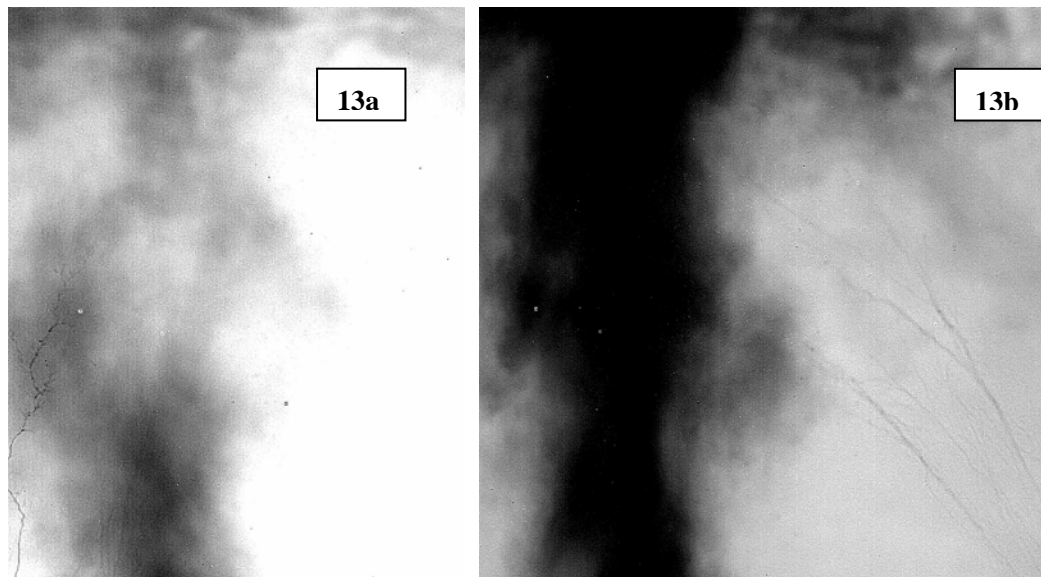


Fig. 12. Both frames show the central part of the aerosol jet. The right frame (18b) indicates that the *stalkers* in the form of brooms reach the jet axis and do not cross it. The left frame (18a) indicates that the positive spark discharge rises from the other side of the jet without crossing it and the *stalkers* are seen in the center. The frame is taken by an IR camera. Exposure time is 7 ms. The number of pixels in each frame is 640x520.

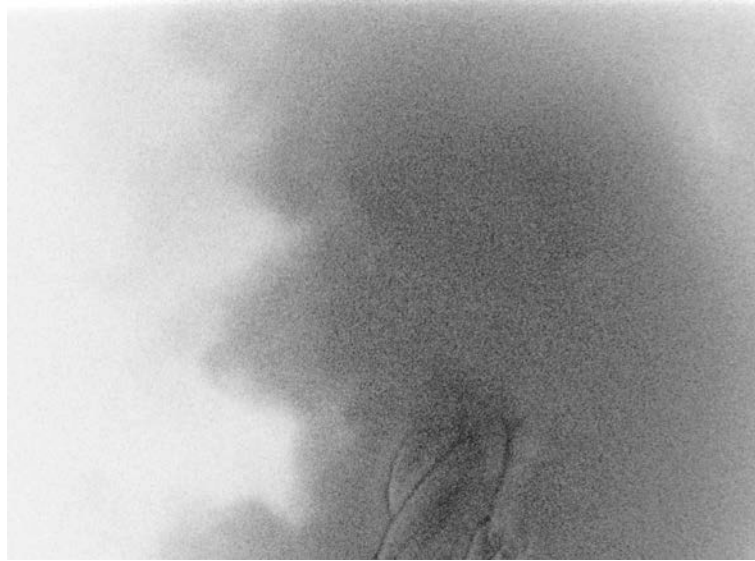


Fig. 13. The visible image taken by a 4 Picos camera aimed at the center of the aerosol cloud at a height of 80-120 cm above the plane where the ball is located. The camera was started by the current coming from the ball through the shunt 400 ns after the initial corona flare. Exposure time is 1 μ s. The image is blurred since the *stalkers* are inside the cloud.

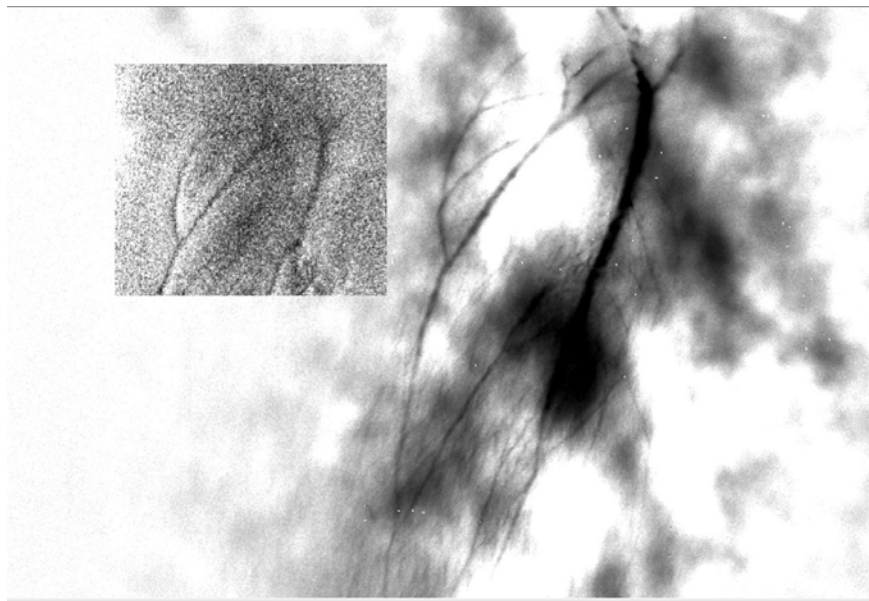


Fig. 14. Simultaneous IR image of the event recorded in Fig. 13. Exposure time of the FLIR 7700M camera is 8 ms. Shown in the upper left corner is a fragment of Figure 13 depicting *stalkers* in the visible range. It can be seen that the contours of the brightest *stalkers* are similar in both images.



Fig. 15. The visible image taken by a 4 Picos camera, which includes both the starting leader a few centimeters long, with the streamer corona rising from the leader, and much less bright plasma structures on the top of the streamer corona, which can be *stalkers*. The camera was started by the current pulse from the ball going through the shunt 400 ns after the initial corona flare. Exposure time is 200 ns.



Fig. 16. The visible image taken by a 4 Picos camera aimed at the center of the aerosol cloud at a height of 80-120 cm above the plane, where the ball from which the discharge started is located. The camera was started by the current pulse with the ball going through the shunt 800 ns after the initial corona flare. Exposure time is 200 ns.